ORIGINAL ARTICLE

Final rubbery state characterization using a hollow cylinder dynamic shear sample on DMA7

Vilaiporn Luksameevanish[1] and Manus Seadan[2]

Abstract

Luksameevanish, V. and Seadan, M.
Final rubbery state characterization using a hollow cylinder dynamic shear sample on DMA7
Songklanakarin J. Sci. Technol., 2004, 26(5) : 637-647

Dynamic properties of raw natural rubber were examined using a hollow cylinder shaped sample subjected to shear deformation on a laboratory Dynamic Mechanical Analyser. According to Cox-Merz's study, dynamic complex viscosity obtained by this method showed a good agreement with shear flow viscosity measured by capillary rheometer. A master curve derived from the dynamic properties were then characterized. A crossing point of storage modulus (G') and loss modulus (G") curves in the master curves was used to identify the final rubbery state, which indicated the transition of rubbery state and molten state. The position of this point depends on quantities and types of reinforcing or non-reinforcing fillers. The final rubbery state was shifted to higher frequency or lower temperature. It was found that the final rubbery state of $CaCO_3$-filled rubber compounds was shifted to higher frequency or lower temperature by approximately 4 decades, while the translation of carbon black-filled rubber compounds was lower than unfilled rubber by about 1 decade. This phenomenon can be used to explain rubber elasticity, i.e. a decreasing of die swell of $CaCO_3$ filled compounds at any high processing temperature. On the other hand, high magnitude of die swell for carbon black filled compound was still obtained.

Key words : dynamic properties, hollow cylinder shear test, raw rubber, master curve, final rubbery state

[1]Ph.D.(Rubber and Polymer Technology), Asst. Prof, [2]Doctorat (Physicochimie des Materiaux Macromoleculaires), Assoc. Prof., Department of Science, Faculty of Science and Technology, Prince of Songkla University, Pattani Campus, Pattani, 94000 Thailand
Corresponding e-mail: vnoparat@bunga.pn.psu.ac.th, mseadan@bunga.pn.psu.ac.th
Received, 8 March 2004 Accepted, 3 June 2004

บทคัดย่อ

วิไลพร ลักษมีวาณิชย์ และ มนัส แซ่ด่าน

การวิเคราะห์หาสภาวะสุดท้ายของสถานะยางด้วยการทดสอบชิ้นตัวอย่างรูปทรงกระบอกกลวงแบบเฉือนบนเครื่อง DMA7

ว. สงขลานครินทร์ วทท. 2547 26(5) : 637-647

สมบัติพลวัตเชิงกลของยางธรรมชาติดิบทดสอบด้วยเครื่องทดสอบพลวัตเชิงกล โดยชิ้นตัวอย่างขึ้นรูปเป็นแบบทรงกระบอกกลวงและมีการผิดรูปแบบเฉือน ผลการทดสอบแสดงให้เห็นว่าค่าความหนืดเชิงซ้อนสอดคล้องกับค่าความหนืดเฉือนที่ได้จากการทดสอบด้วยเครื่องคาปิลารีรีโอมิเตอร์และสอดคล้องกับผลการศึกษาของ Cox และ Merz จากนั้นจึงวิเคราะห์หากราฟหลักของสมบัติพลวัตที่ทดสอบได้ จากกราฟหลักดังกล่าวทำให้สามารถกำหนดสภาวะสุดท้ายของสถานะยาง (final rubbery state) จากจุดตัดของค่ามอดุลัสสะสม (Storage modulus, G') และมอดุลัสสูญ (Loss modulus, G") สภาวะสุดท้ายของสถานะยางนี้เป็นจุดแยกสถานะยาง (rubber state) ออกจากสถานะยางหลอม (molten state) ที่ขึ้นกับปริมาณและชนิดของสารตัวเติมแบบเสริมแรงหรือไม่เสริมแรง เมื่อเทียบกับยางที่ไม่มีสารตัวเติมผสม พบว่ายางผสม $CaCO_3$ มีสภาวะสุดท้ายของสถานะยางเลื่อนไปยังความถี่สูงขึ้นประมาณ 4 อันดับ ในขณะที่เขม่าดำทำให้สภาวะนี้เลื่อนไปน้อยกว่า 1 อันดับ ปรากฏการณ์นี้ใช้อธิบายสมบัติยืดหยุ่นของยาง เช่น การบวมพองที่หัวไดน์ลดลงเมื่อใช้ยางผสม $CaCO_3$ ในกระบวนการผลิตที่อุณหภูมิสูงใด ๆ ในทางตรงกันข้าม การบวมพองที่หัวไดน์ยังคงมีค่าสูงเมื่อใช้ยางผสมเขม่าดำ

ภาควิชาวิทยาศาสตร์ คณะวิทยาศาสตร์และเทคโนโลยี มหาวิทยาลัยสงขลานครินทร์ อำเภอเมือง จังหวัดปัตตานี 94000

The frequency and temperature dependence of dynamic properties for viscoelastic materials are well known (Nilsen, 1974, Freakley and Payne 1978, Jones 1991 and Fried, 1995). In general, dynamic tests are nondestructive and can be performed over a limited range of frequency or temperature, depending upon equipment and technique. There are some difficulties in preparing a sample that can be held over a wide temperature range, in which the material can be changed from a solid (glassy) state to a melt state. Conventionally, complex modulus data (i.e. storage modulus, loss modulus and tan δ) have been measured over a range of temperatures and frequencies from the test as shown in Figure 1 (Jones, 1991). However, it is possible to display these data in such a way that the effects of each parameter are individually combined into a single variable (Jones, 1991) and presented as a "master curve".

The "master curve" generally transfers data from various tested temperatures to one reference temperature by moving the data on the log scale of frequency axis (Jones, 1991). If the originally measured modulus or tan δ varying with frequency (f) at each absolute temperature (T) are denoted as G(f,T) and ϑ(f,T) respectively, the corresponding parameters at the reduced frequency, f_r, are $G(f_r)$ and $\vartheta(f_r)$. The relationships between the measured data and reduced data set are as follows (Jones, 1991).

The data transfer:

$$G(f,T) = \frac{To\rho o}{T\rho} G(f_r) \quad (1)$$

$$\vartheta(f,T) = \vartheta(f_r) \quad (2)$$

The frequency transfer :

$$f_r = f * a_T \quad (3)$$

or $$a_T = \frac{f}{f_r} \quad (4)$$

where a_T is a "shift factor" which is a function of absolute temperature, T, relative to a chosen reference temperature T_0. Equation (4) shows that a_T is a ratio of shifted frequency at

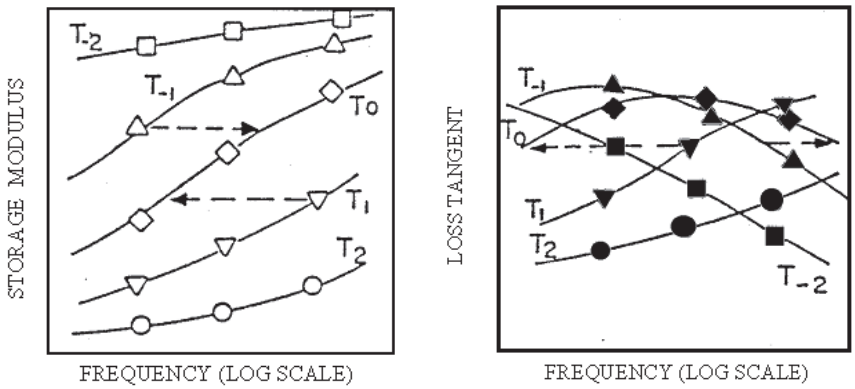

Figure 1. Idealized storage modulus and loss tangent as a function of frequency at various temperatures for a viscoelastic material (after Jones, 1991)

temperature T over a reference frequency at temperature T_0. In most cases, $T\rho o/T\rho$ does not differ greatly from unity over a wide temperature range and the difference is usually negligible in comparison with the data scatter due to other sources of error (Jones, 1991). The shift factor can be estimated in many ways, including manual estimation on a temperature by temperature basis, statistical analysis of repeated manual estimates, and fitting of assumed functions by minimization of least square errors (Jones, 1991). The most popular equation is the WLF equation as followed.

Williams-Landel-Ferry (WLF) relation:

$$\log a_T = \frac{-C_1(T - T_0)}{C_2 + (T - T_0)}$$

For any type of polymer, the master curve of storage modulus (G'), loss modulus (G") and tan δ can be drawn as shown in Figure 2 (a). As can be seen from this figure, four main regions have been identified and classified as the glassy, transition, rubbery elastic, and flow region. The storage modulus of viscoelastic material decreases continuously with decreasing frequency or increasing temperature, corresponding to the changed from the glassy to the flow region. In the transition region, dramatic changes in all three properties, (i.e. G', G" and tan δ) are clearly observed. In the flow region, the rate of decrease of the storage modulus is greater than that of the loss modulus. Thus, this causes the value of loss modulus to be greater than the storage modulus in the extreme flow region.

In processing equipment such as an extruder, injection moulding or compression mould machine, rubber is usually heated or given a reduced frequency in order to flow in the flow region. Considering Figure 2 (b), the elastic property can be dominate, providing that G' is greater than G". Operating at this condition, products can be disordered from the elastic effect such as a die swell, a bamboo effect or a shark skin phenomena. This effect will disappear if the processing condition moves to a flow state, where the value of G' is lower than G". Therefore, a final rubbery state is then defined here as the crossing point of G' and G".

This work aimed to characterize the final rubbery state of raw natural rubber using a hollow cylinder sample tested under shear mode on the Dynamic Mechanic Analysis series 7 (DMA7). The effect of types and amounts of fillers on the final rubbery state were also examined. This state can be used to predict the behaviour of rubber compounds in processing processes.

Material and Methods

This work was divided into two main parts of (i) an examination of the test method and (ii) the determination of a master curve. The first part

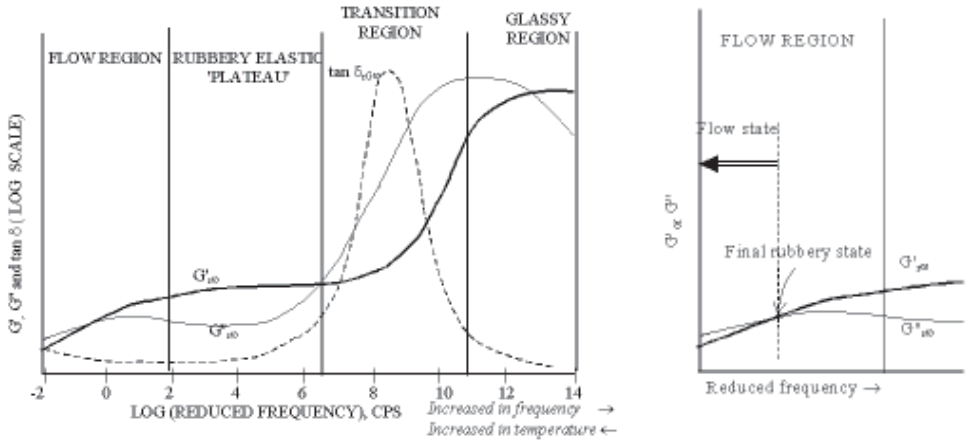

(a) **(b)**

Figure 2. Diagram of (a) master curve of storage modulus, loss modulus and tan δ of polymer (after Freakley, P.K. and Payne, A.R, 1978) and (b) the final rubbery state.

was to design a sample that can be subjected to dynamic load over a wide temperature range in which the rubber will be changed from rubbery to molten state. Reliable results must also be evaluated (Noparatanakailas and Seadan, 2000). The master curves were determined in the second part to indicate the final rubbery state of each rubber compounds.

Part I: Examination of test method

A hollow cylinder sample was designed to test raw rubber by using the Dynamic Mechanic Analyser series 7 (DMA7) machine manufactured by Perkin Elmer. Figure 3 shows a diagram of the sample geometry and sample preparation. Tests were performed at a frequency range from 0.1 to 50 Hz and at a certain temperature of 100ºC. Four grades of raw natural rubber, namely STR5L, STR20, RSS and skim block were used.

In order to validate the results, the dynamic viscosity was compared with the shear flow viscosity measured on a standard capillary rheometer. The complex viscosity, noted as η*(ω), was calculated from the following relation (Ferry, 1962).

$$\eta^*(\omega) = \sqrt{\left(\frac{G'}{\omega}\right)^2 + \left(\frac{G''}{\omega}\right)^2}$$

where G' and G" are the storage and loss modulus at angular frequency ω (ω=2πf), respectively.

The flow viscosity, noted as $\eta(\dot{\gamma})$, was obtained from the extrusion method using the Rosand capillary rheometer. Based on the equivalent of the shear rate and the angular frequency ($\dot{\gamma}$= ω), following Cox and Merz's assumption (Cox and Merz, 1962 and Cox and Merz, 1971), the comparison was taken.

Part II: Determination of master curve

The dynamic behavior of three sets of materials was examined, namely STR5L, STR5L mixed with carbon black grade N330, and STR5L mixed with calcium carbonate ($CaCO_3$). The available frequency range of 0.1 to 50 Hz was selected. For STR5L the temperatures of 100, 120, 140, 160, 180 and 200ºC were chosen. The STR5L rubber was mixed with different amounts of N330-black: 20, 40 and 60 phr, using a two-roll mill. The STR5L and N330-black compounds were tested at the temperatures of 80, 120, 160 and 200ºC. For the compounds containing $CaCO_3$: 5, 10, 20, 40 and 60 phr, the test temperatures were changed in step mode over the range between 80 and 200ºC. With the 5 and 10 phr of $CaCO_3$ compounds, the temperatures up to 200ºC could be used for the

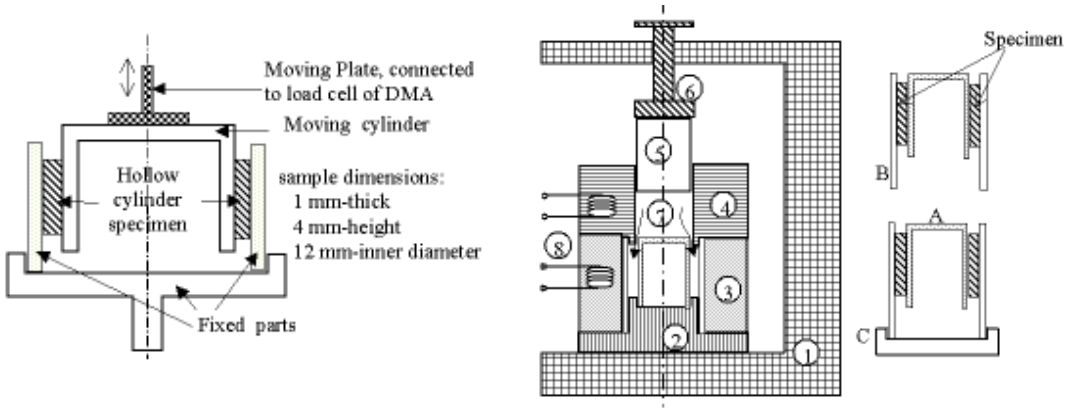

(a) **(b)**

Figure 3. Side view of (a) a hollow cylinder specimen and (b) sample preparation components. Note: A and B are an inner and outer metal holder cylinder respectively. C is a supported metal plate. 1 is a metal clamp, holding the whole set. 2 is a lower part of the mould, holding a molten rubber. 3 is a surrounded hollow cylinder, where the heat is supplied. 4 is a heated barrel used to collect rubber melts. 5 is a piston. 6 is a plate used to drive the piston. 7 is rubber melt. 8 is electric heater wires.

testing. The maximum workable test temperature of testing the 20 and 40 phr of the $CaCO_3$ compounds was 160ºC while the temperature for the 60 phr filled compound was 140ºC. The limitation of temperature used for the 60 phr $CaCO_3$ containing compound was due to a softening of the compounds.

In order to construct a master curve, data were collected at a reference temperature of 120ºC for all of the conditions of materials and frequencies. A shift movement of measured G' and G'' values was done only in the log ω axis (x-axis), by using a reduced frequency as follows: Firstly, a set of frequency data at each temperature corresponding to a given set of G' data were extracted from the raw data. For each value of G', a ratio of f_r (frequency at the reference temperature) and f (frequency at any temperature) was determined and defined as a shift factor (a_T) for a specific temperature. The average value of a_T over the given set of G' data was then calculated. Considering the WLF equation, rewritten as Equation (5), the constants (C_1 and C_2) were calculated. The relationship between $(T-T_0)/\log a_T$ and $(T-T_0)$ is linear. Therefore, C_1 and C_2 were related to the slope and intercept values of the curve; C_1 = -1/slope, and C_2 = -intercept x C_1. This linear relationship between $(T-T_0)/\log a_T$ and $(T-T_0)$ was calculated using Microsoft Excel software. Finally, the storage modulus, G' and loss modulus, G'' (in Pa) were plotted with the reduced frequency, ωa_T, at each temperature on a log-log scale.

WLF equation:

$$\log a_T = \frac{-C_1(T-T_0)}{C_2+(T-T_0)}^{\#}$$

$$\frac{(T-T_0)}{\log a_T} = -\frac{C_2}{C_1}-\frac{1}{C_1}(T-T_0) \qquad (5)$$

Results and Discussion

Part I: Examination of test method

Four grades of natural rubbers; STR5L, STR20, RSS and skim block having a money

---

[#] **From this equation, (T-To) can be considered in degrees Celsius.**

viscosity of 74 MV, 85MV, 92 MV and 80 MV, respectively, were tested at 100ºC and 0.5% strain over the frequency range 0.1 to 50 Hz. The complex viscosity was then calculated in order to compare with the shear flow viscosity, tested from the standard capillary rheometer. Figure 4 (a) shows an insignificant difference in the apparent shear flow viscosity of these four natural rubber grades. The lowest shear rate, obtaining from the test, is about 5 per second. The value of the apparent shear viscosity decreases with an increasing of shear rate. The maximum viscosity of rubber is about $1.5x10^4$ Pa.s at the shear rate of 5/s. Figure 4 (b) shows that the shear flow viscosity as a function of shear rate is almost identical to the complex viscosity as a function of angular frequency. This is in accordance with a study by Cox and Merz's (1962 and 1971). There is also not much difference in the complex viscosity of the four rubber grades. The dynamic testing can be operated at a lower rate of deformation than that of the capillary method. Therefore, the shear testing of raw natural rubber as a hollow cylinder on the DMA7 is an valid method, which provides consistent and reliable data.

Part II: Determination of master curve

Raw data of G' and G" in Pascal varying over a frequency range of 0.1-50 Hz are plotted on a log-log scale with the angular frequency. An

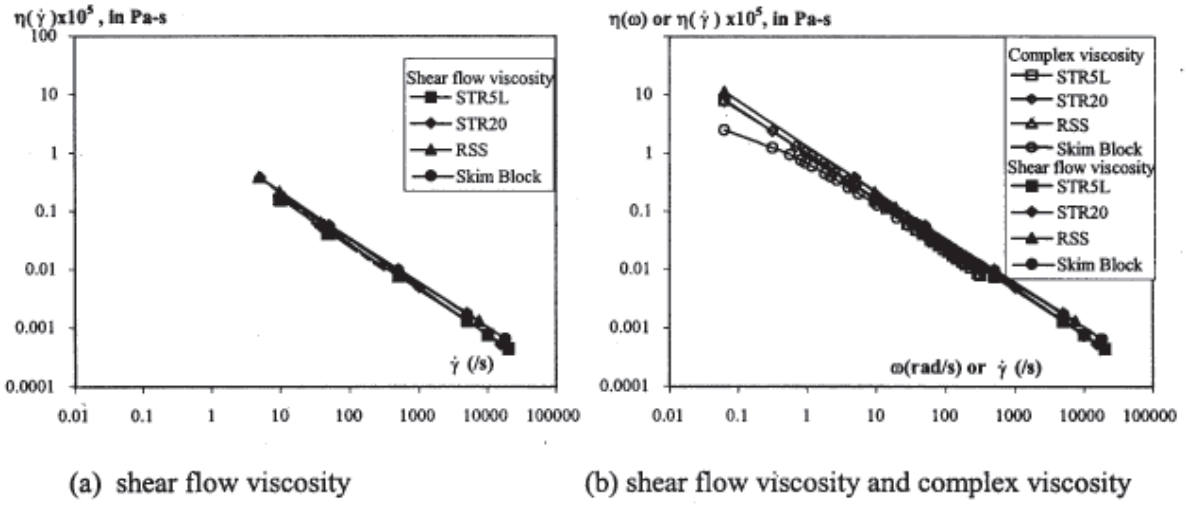

Figure 4. Comparison of complex viscosity ($\eta^*(\omega)$) and shear viscosity ($\eta(\dot{\gamma})$) at 100ºC.

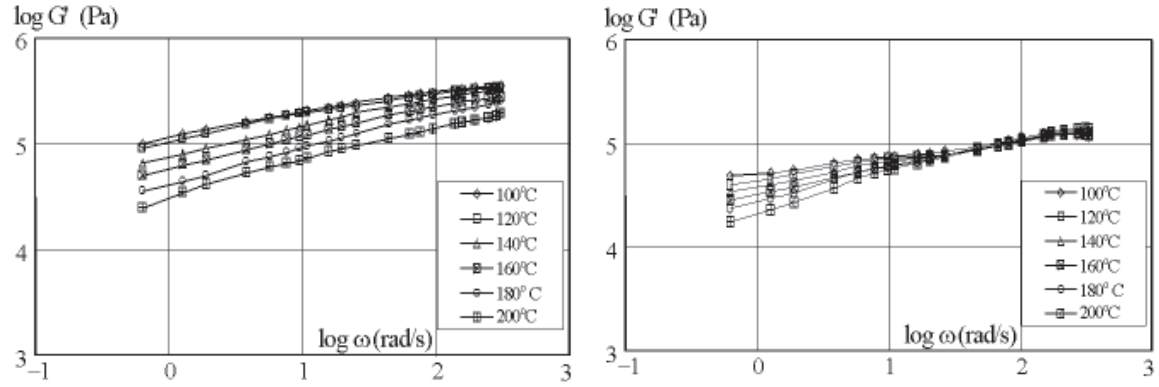

Figure 5. Storage and loss modulus of STR5L tested at 100, 120, 140, 160, 180 and 200ºC.

Table 1. Example of STR5L frequency tabulation for a_T and the WLF constants evaluation.

Given G' (Pa)	f (Hz)							(T-T_0)(ºC)					
	100ºC	120ºC (T_0)	140ºC	160ºC	180ºC	200ºC		-20	0	20	40	60	80
1.70E+05	0.3	**0.9**	2.2	5	7	16		3.00	1.00	0.41	0.18	0.13	0.06
1.80E+05	0.4	**1.1**	2.7	6	9	24		2.75	1.00	0.41	0.18	0.12	0.05
1.90E+05	0.6	**1.4**	3.5	7	13	27	$a_T = f(T_0)/f(T)$	2.33	1.00	0.40	0.20	0.11	0.05
.	.	.	.	.	.	.		.	.	.	.	.	.
.	.	.	.	.	.	.		.	.	.	.	.	.
.	.	.	.	.	.	.		.	.	.	.	.	.
2.40E+05	2.7	**6**	9	20	39	2.22		1.00	0.67	0.30	0.15		
2.50E+05	3.2	**7**	11	24	43	2.19		1.00	0.64	0.29	0.16		
							Average a_T	**2.37**	**1.00**	**0.51**	**0.22**	**0.12**	**0.06**
							Log a_T	**0.37**	**0.00**	**-0.29**	**-0.65**	**-0.91**	**-1.21**
							-(T-To)/(Log a_T)	**-53.36**		**-68.51**	**-61.52**	**-66.15**	**-65.99**
							Slope of the -(T-To)/(Log a_T) versus (T-To) curve, m	-0.11					
							Intercept of the -(T-To)/(Log a_T) versus (T-To) curve, b	-59.14					
							C_1 = -1/m	**9.09**					
							C_2 = -b/m	**537.6**					

Table 2. Shift factors and WLF constants.

	a_T at temperature							C_1	C_2
	80ºC	100ºC	120ºC	140ºC	160ºC	180ºC	200ºC		
Reference (Ferry, 1962)	5.09	2.10	1.00	0.53	0.31	0.19	0.13	3.65	246.6
STR 5L	-	2.37	1.00	0.51	0.22	0.12	0.06	9.09	537.6
STR 5L + N-330 20 phr	5.05	-	1.00	-	0.22	-	0.06	16.95	1001.0
STR 5L + N-330 40 phr	3.59	-	1.00	-	0.30	-	0.10	14.53	1081.0
STR 5L + N-330 60 phr	2.97	-	1.00	-	0.38	-	0.15	9.53	849.9
STR 5L + $CaCO_3$ 5 phr	4.94	-	1.00	-	0.23	-	0.08	8.20	502.4
STR 5L + $CaCO_3$ 10 phr	4.35	-	1.00	-	0.36	-	0.07	9.35	670.8
STR 5L + $CaCO_3$ 20 phr	-	2.53	1.00	0.32	0.21	-	-	9.62	465.1
STR 5L + $CaCO_3$ 40 phr	-	2.31	1.00	0.39	0.26	-	-	6.25	344.1
STR 5L + $CaCO_3$ 60 phr	3.69	1.96	1.00	0.55	-	-	-	8.00	590.1

example of the raw data is shown in Figure 5 for STR5L. It is clearly seen that G' and G" values of STR5L increase with increasing frequency and reduce with increasing temperature over the range 100 to 200ºC. Table 1 provides an example of frequency data for a given set of G' values and test temperatures for STR5L. This table gives the evaluation of a_T, the slope and intercept of the linear relation of (T-T_0)/log a_T plotted against (T-T_0), and the WLF constants, C_1 and C_2. The results in terms of a_T and the WLF constants, for all the studied cases, are shown in Table 2, which also includes the reference values of natural rubber (Ferry, 1962). The experimental values of a_T, especially for STR5L, agree well with the reference values at five temperatures of 100, 140, 160, 180 and 200ºC. The values of C_1 and C_2 obtained here are in the same order of the reference ones. Figure

6 shows the plot of shift factor, a_T, for all experimental data and the reference values, varying with temperature. It shows good agreement between the a_T values obtained from this present study and those documented in the literature (Ferry, 1962). This confirms the reliabilities of experimental data for determining the master curves of G' and G".

The experimental data, G' and G", tested at various temperatures (from 80 to 200ºC) were shifted in the frequency axis to the reference temperature (120ºC), using the corresponding shift factor, a_T. Single lines of G' and G", plotted against the reduced frequency ωa_T, were obtained and are shown as examples in Figure 7 for STR5L, STR5L + 40phr N330, and STR5L + 40phr $CaCO_3$. The average value of G' and G" are plotted as solid lines, while the experimental data are presented as symbols shown for each cases.

Figure 8 shows the average master curves of G' and G" for all of the experimental cases. These curves vary with the widest reduced frequency range of about 6 decades of log ωa_T. From this figure, the influence of filler on the value of modulus and on the movement of the final rubbery state along the x-axis can be clearly seen. N330-black is a reinforcing filler, and causes both G' and G" values to increase as a consequence of increasing filler amount (Figure 8(a)). On the other hand, the $CaCO_3$, which is a non-reinforcing filler, softens the compound (Figure 8(b)). The final rubbery state of STR5L is located at the approximate reduced frequency of -1.5. The addition of carbon black or $CaCO_3$ causes a movement of the crossing point to a higher value of the reduced frequency. The amount of carbon black causes insignificant difference in the movement of the crossing point. The crossing point of G' and G" moves from -1.5 (for STR5L) to around -0.5 to -0.2 (for the N-300 mixed up to 60 phr) or about 1 decade. A large movement of this crossing point, of around 3 to 4 decades, is seen in the case of 60 phr-$CaCO_3$ mixing.

The use of the final rubbery state characteristics on the rubber processing can be described as follows. For example, a compound of STR5L mixed with 40 phr $CaCO_3$ is extruded at a constant shear speed of 100/s. According to the characteristic curve shown in Figure 8(b), if the operation temperature is 120ºC, the value of G' is greater than the value of G" when log $\omega a_T = 2$ (equivalent of shear speed of 100/s). Therefore, the elastic effect on the products will occur. This phenomenon will disappear, if the operation temperature is higher. By using the time-temperature super-

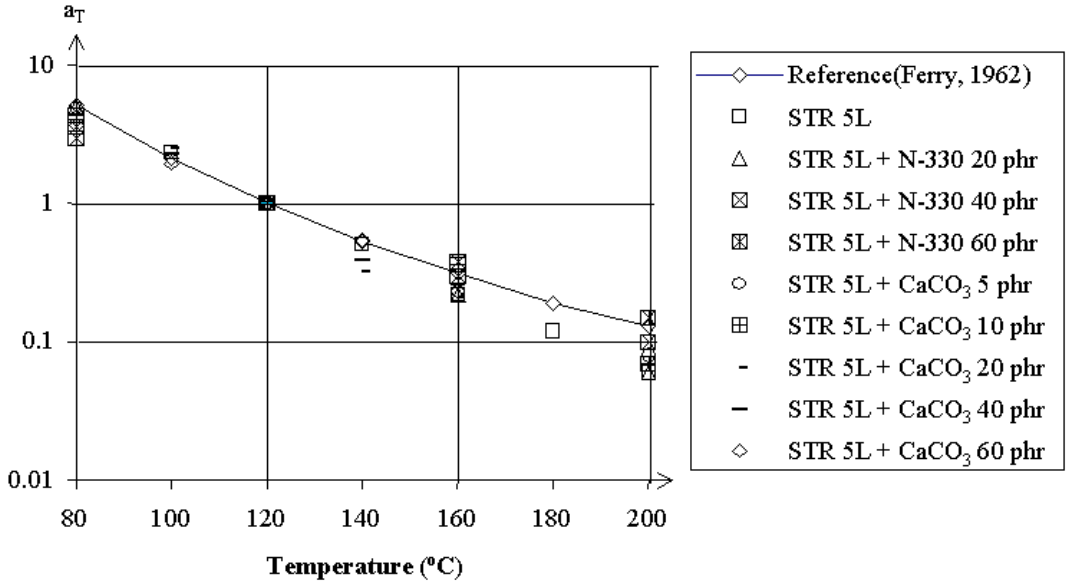

Figure 6. A plot of a_T against temperature for all cases.

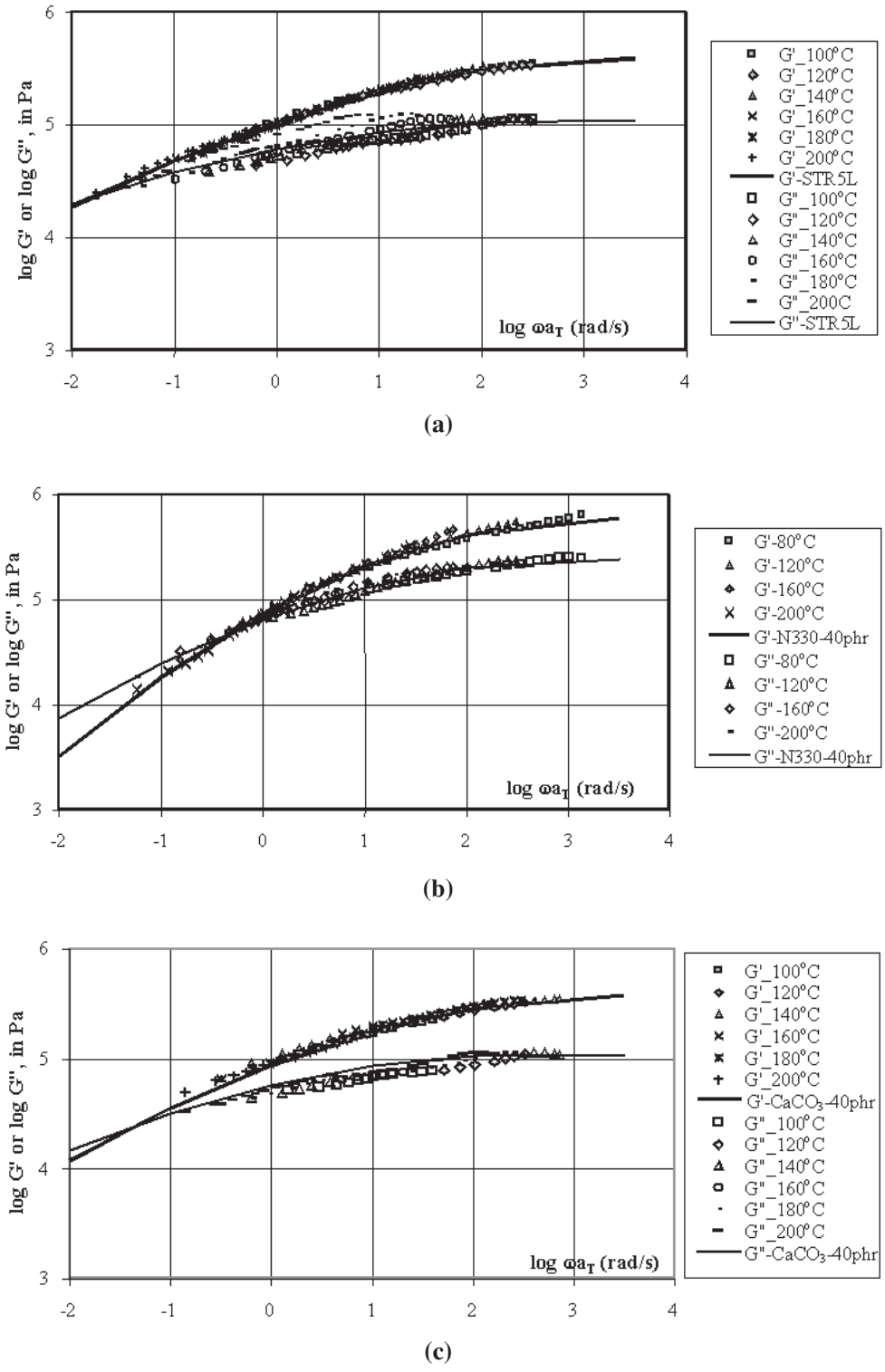

Figure 7. Master curves of (a) STR5L, (b) STR5L+40phr of N330 and (c) STR5L + 40 phr of $CaCO_3$. The reference temperature used is 120ºC.

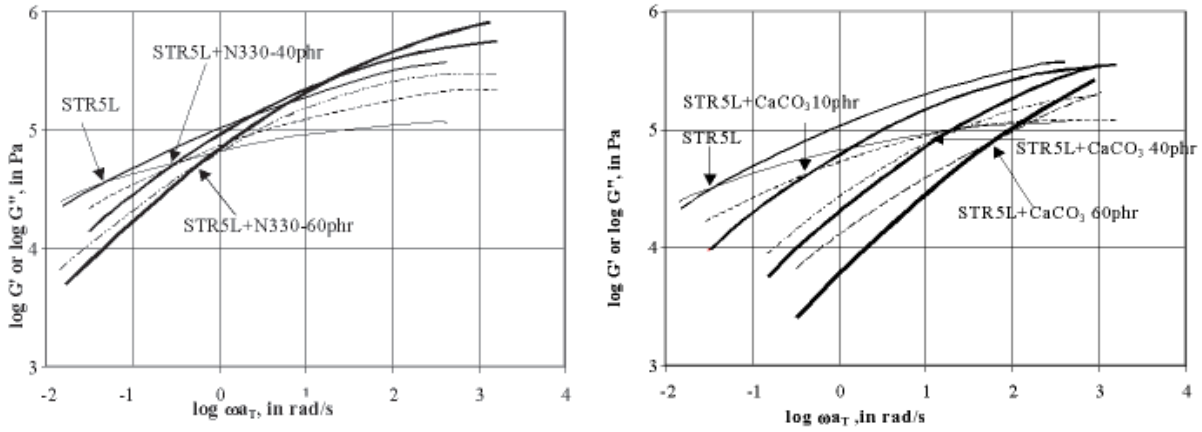

(a) **(b)**

Figure 8. Effect of filler type and amount on master curve: (a) STR5L and STR5L+N330 and (b) STR5L + $CaCO_3$. The bold lines present storage modulus while light or dot lines are loss modulus.

position method, the operating frequency must be shifted to a lower frequency where log ωa_T is equal to 1, the final rubbery state of this case (see Figure 8(b)). The reducing of this shift factor must be equal to 1 decade (from operating point log ωa_T = 2 to the final rubbery state, log ωa_T =1). Considering Figure 6, the lower value of shift factor of 1 decade is equal to the increase of temperature from 120ºC to about 180ºC.

Conclusion

In this study, a hollow cylinder shear sample is presented as an appropriate test for dynamic properties characterization of raw rubber on the DMA7 with limited range of sample stiffness and temperature of testing. Samples with high stiffness, such as a high content of reinforcing filler or testing at low temperatures, were not studied because of the limitation of the machine. Samples of overt softness, such as a high content of non-reinforcing filler, or testing material at temperatures approaching a molten temperature could not be studied because of softening of the samples, which no longer appeared as a cylindrical specimen.

The master curves of storage modulus and loss modulus can be obtained by the Time-Temperature superposition method and give the final rubbery state of each cases. The final rubbery state of the compound depends greatly on type and amount of filler. The reinforcing filler, N330-black causes a higher value in both G' and G" since it brings about a stiffness effect. The final rubbery state shifts to a higher value of the reduced frequency for only about 1 decade in case of 60 phr. So, this compound still have an influence of elastic effect during the processing similar to the unfilled rubber. On the other hand, the non-reinforcing filler, $CaCO_3$, softens the compound and causes a large movement of the final rubbery state. In the case of the 60 phr-$CaCO_3$ blend, the magnitude of this movement is around 3 to 4 decades. Therefore, less elastic effect will be seen in the 60 phr-$CaCO_3$ compound.

Acknowledgment

This study would not be complete without the B.Sc. work of Miss. T. Sukpilap, Mr. U. Tongyu and Mr. A. Wongsuwang; the authors extend great thanks to you all.

References

Cox, W.P. and Merz, E.H. 1962. **In**: Nielsen, L.E., Mechanical Properties of Polymers, Reinhold Publishing Corp., London, UK., pp.205-207.

Cox, W.P. and Merz, E.H. 1971. **In**: William, D.J., Polymer Science and Engineering, Prentice-Hall, Inc., New York, USA., pp. 298-311.

Ferry, J.D. 1962. Viscoelastic Properties of Polymers, John Wiley & Sons, Inc., New Jersey, USA. pp. 1-12 and pp.292-318.

Freakley, P.K. and Payne, A.R. 1978. Theory and Practice of Engineering with Rubber. Applied Science Publishers Ltd., Great Yarmonth, UK., pp.56-109.

Fried, J.R. 1995. Polymer Science and Technology, Pretice-Hall, International Inc., New Jersey, USA. pp.182-218.

Jones, D.I.G. 1991. Behaviour of Polymeric Material for Damping Applications, Fundamentals of Damping Technology an Applications for Vibration Suppression. San Diego, CA, 11-12 February 1991.

Nielsen, L.E. 1974. Mechanical Properties of Polymers, Reinhold Publishing, Corp., New York, USA. pp.139-160.

Noparatanakailas, V. and Seadan, M. 2000. Hollow cylinder sample test using a dynamic mechanical analyser. J of Rub Res, 3(2): 95-103.